JEMAT 2022, Vol 10, No 1, 23-27
https://doi.org/10.54987/jemat.v10i1.694

HIBISCUS PUBLISHER

JOURNAL OF ENVIRONMENTAL MICROBIOLOGY AND TOXICOLOGY

Website: http://journal.hibiscuspublisher.com/index.php/JEMAT/index

Isothermal Modelling of the Adsorption of Lead(II) Onto an Antarctic Sea-Ice Bacterial Exopolysaccharide

Muhammed Abdullahi Ubana[1], Murtala Ya'u[2], Hartinie Marbawi[3], Nur Adeela Yasid[1]* and Mohd Yunus Shukor[1]

[1]Department of Biochemistry, Faculty of Biotechnology and Biomolecular Sciences, Universiti Putra Malaysia, 43400 UPM Serdang, Selangor, D.E, Malaysia.
[2]Department of Biochemistry, Faculty of Basic Medical Sciences, College of Health Sciences, Bayero University Kano, Nigeria.
[3]Biotechnology Programme, Faculty of Science and Natural Resources, Universiti Malaysia Sabah, 88400 Kota Kinabalu, Sabah.

*Corresponding author:
Nur Adeela Yasid
Department of Biochemistry,
Faculty of Biotechnology and Biomolecular Sciences,
Universiti Putra Malaysia,
43400 UPM Serdang,
Selangor, D.E,
Malaysia.
Email: adeela@upm.edu.my

HISTORY

Received: 23rd April 2022
Received in revised form: 24th June 2022
Accepted: 21st July 2022

KEYWORDS

Biosorption
Lead (II)
Isotherm
Antarctic sea-ice bacterial exopolysaccharide , Sips

ABSTRACT

The biosorption of the biosorption of lead(II) onto an Antarctic sea-ice bacterial exopolysaccharide is remodeled using nonlinear regression and the optimal mode was determined by a series of error function assessments. The Sips model performed best in statistical tests including root-mean-square error (RMSE), adjusted coefficient of determination (adjR^2), bias factor (BF), accuracy factor (AF), and corrected Akaike Information Criterion (AICc) which is not the same to the originally published work using a linearized form where the Langmuir and Freundlich models best represent the biosorption and the maximum biosorption capacity. The calculated Sips parameters k_S (l/g) value of 0.10 (95% confidence interval from 0.08 to 0.13), a maximum monolayer adsorption capacity q_{mS} (mg/g) value of 252.88 (95% C.I. from 222.13 to 283.64) and n_S (Sips model exponent) value of 1.16 (95% C.I. from 1.34 to 1.98). This study indicates that a different isotherm model can be obtained using nonlinear regression compared to the popular linearized form that may give relatively inaccurate outcome.

INTRODUCTION

Heavy metals are increasingly being released into the environment as a byproduct of mining, electroplating, alloy preparation, pulp-paper, and fertilizer production, among other industrial processes. The issue of pollution involving heavy metals is of paramount importance due to the accumulation of heavy metals in the food chain and the severe health concerns they cause to living beings. Lead is a naturally occurring toxic element found in the Earth's crust. Polluting large areas, exposing large numbers of people, and negatively impacting public health are all direct results of its widespread use in a variety of countries. More than 75% of all lead is used in the production of lead-acid car batteries. But lead is also used in many other products, such as pigments, paints, solder, stained glass, lead crystal glassware, ammunition, ceramic glazes, jewelry, toys, cosmetics, and traditional medicines. If the water pipes themselves are made of lead or if the pipes are joined together with lead-based solder, then the water you drink may contain lead. The majority of lead in international trade today is derived from recycled materials. Lead's negative effects on children are more severe because their developing brains and nervous systems are more susceptible to its toxicity. Adults who are exposed to high levels of lead are more likely to develop hypertension and kidney damage. Lead exposure is dangerous for everyone, but it can have devastating effects on pregnant women and their babies [1–3]. Anemia, hepatitis, encephalopathy, and nephritic syndrome have all been linked to lead levels in drinking water that are above the legal limit of 0.05 mg/L. Due to its high biosorption capacity and selectivity, low cost, and low environmental risk, biosorption is a promising approach for the removal of heavy metals from wastewater [1–3].

Exopolysaccharide or EPS is secreted by a number of Antarctic microorganisms as a defense mechanism against the bitter cold and concentrated salt air. Hyposaline conditions are created when ice melts, exposing bacteria that have been trapped in the ice to the ocean below. Antarctic EPSs likely played an important role in protecting organisms living within ice floes from ice-crystal damage, buffering against pH and salinity fluctuations, and relieving other chemical stresses like heavy metals , though the mechanism was not so evident. It has been

shown sea-ice isolates have EPSs with molecular weights that are five- to fifty-times higher than those produced by other marine isolates [4]. EPSs formed by sea-ice isolates may function as promising biosorbents for heavy metals removal in saltwater treatment because of their appealing structure and physicochemical features [5].

It is critical to correctly assign the kinetics and isotherms of biosorption in order to comprehend the biosorption process of toxicants. Estimating uncertainty of the parameters of the kinetics, which are often displayed as a 95 percent confidence interval range, can be made more challenging by the linearization of a clearly nonlinear curve, which can cause problems on the error structure of the data [6]. Error in the independent variable might also be introduced during data transformation for linearization. In addition, the fitted parameter values for the linear and nonlinear variants of the model can differ due to changes in the weight placed on each data point [7]. In this study the published data from the biosorption of lead(II) onto an Antarctic sea-ice bacterial exopolysaccharide [5] is remodeled using nonlinear regression of several isothermal models (**Table 1)** and the optimal mode was determined by a series of error function assessments. Given that the isotherms in the paper were proposed using a linearized modeling version, this modeling analysis was warranted.

Table 1. Isotherm models utilized in this study.

Model	Formula	Ref
Henry's law	$q_e = HC_e$	[8]
Langmuir isotherm	$q_e = \frac{q_{mL} b_L C_e}{1 + b_L C_e}$	[9]
Freundlich isotherm	$q_e = K_F C_e^{\frac{1}{n_F}}$	[10]
Sips isotherm	$q_e = \frac{K_s q_{mS} C_e^{\frac{1}{n_S}}}{1 + K_s C_e^{\frac{1}{n_S}}}$	[11]
Toth isotherm	$q_e = \frac{q_{mT} C_e}{\left(K_T + C_e^{n_T}\right)^{n_T}}$	[12]
BET isotherm	$q_e = \frac{q_{mBET} \alpha_{BET} C_e}{(1 - \beta_{BET} C_e)(1 - \beta_{BET} C_e + \alpha_{BET} C_e)}$	[13]
Baudu isotherm	$q_e = \frac{q_{mB} b_B C_e^{(1+x+y)}}{1 + b_B C_e^{(1+x)}}$	[14]
Fritz-Schlunder-IV isotherm	$q_e = \frac{A_{FS} C_e^{a_{FS}}}{1 + B_{FS} C_e^{b_{FS}}}$	[15]
Fritz-Schlunder-V isotherm	$q_e = \frac{q_{mFS5} K_1 C_e^{\alpha_{FS}}}{1 + K_2 C_e^{\beta_{FS}}}$	[15]

METHODS

Data acquisition and fitting

Data from figure 4 from a published work [5] were digitized using the software Webplotdigitizer 2.5 [16].The accuracy of data digitized with this program has been verified [17,18]. The data were then nonlinearly regressed using the curve-fitting software CurveExpert Professional software (Version 1.6).

Statistical analysis

Commonly used statistical discriminatory methods such as corrected AICc (Akaike Information Criterion), Bayesian Information Criterion (BIC), Hannan and Quinn's Criterion (HQ), Root-Mean-Square Error (RMSE), bias factor (BF), accuracy factor (AF) and adjusted coefficient of determination (R^2).

The RMSE was calculated according to **Eq. (1)**, [6], and smaller number of parameters is expected to give a smaller RMSE values. n is the number of experimental data, Ob_i and Pd_i are the experimental and predicted data while p is the number of parameters.

$$RMSE = \sqrt{\frac{\sum_{i=1}^{n} (Pd_i - Ob_i)^2}{n - p}} \quad \text{(Eqn. 1)}$$

As R^2 or the coefficient of determination ignores the number of parameters in a model, the adjusted R^2 is utilized to overcome this issue. In the equation (**Eqns. 2** and **3**), the total variance of the y-variable is denoted by S_y^2 while RMS is the Residual Mean Square.

$$Adjusted\left(R^2\right) = 1 - \frac{RMS}{s_Y^2} \quad \text{(Eqn. 2)}$$

$$Adjusted\left(R^2\right) = 1 - \frac{\left(1 - R^2\right)(n-1)}{(n - p - 1)} \quad \text{(Eqn. 3)}$$

The Akaike Information Criterion (AIC) is based on the information theory. It balances between the goodness of fit of a particular model and the complexity of a model [19]. To handle data having a high number of parameters or a smaller number of values corrected Akaike information criterion (AICc) is utilized [20]. The AICc is calculated as follows (**Eqn. 4**), where p signifies the quantity of parameters and n signify the quantity of data points. A model with a smaller value of AICc is deemed likely more correct [20].

$$AICc = 2p + n\ln\left(\frac{RSS}{n}\right) + 2(p+1) + \frac{2(p+1)(p+2)}{n-p-2} \quad \text{(Eqn. 4)}$$

Aside from AICc, Bayesian Information Criterion (BIC) (**Eqn. 5**) is another statistical method that is based on information theory. This error function penalizes the number of parameters more strongly than AIC [21].

$$BIC = n.\ln\frac{RSS}{n} + k.\ln(n) \quad \text{(Eqn. 5)}$$

A further error function method based on the information theory is the Hannan–Quinn information criterion (HQC) (**Eqn. 6**). The HQC is strongly consistent unlike AIC due to the ln ln n term in the equation [20];

$$HQC = n \times ln\frac{RSS}{n} + 2 \times k \times ln(\ln n) \quad \text{(Eqn. 6)}$$

Further error function analysis that originates from the work of Ross [22] are the Accuracy Factor (AF) and Bias Factor (BF). These error functions test the statistical evaluation of models for the goodness-of-fit but do not penalize for number of parameter (**Eqns. 7 and 8**).

$$\text{Bias factor} = 10^{\left(\frac{\sum_{i=1}^{n}\log\frac{(Pd_i/Ob_i)}{n}}{n}\right)} \quad \text{(Eqn. 7)}$$

$$\text{Accuracy factor} = 10^{\left(\frac{\sum_{i=1}^{n}\log\frac{|(Pd_i/Ob_i)|}{n}}{n}\right)} \quad \text{(Eqn. 8)}$$

RESULTS AND DISCUSSION

The equilibrium data from [5] was analyzed using nine models—Henry, Langmuir, Freundlich, BET, Toth, Sips, Fritz-Schlunder IV, Baudu and Fritz-Schlunder V, and fitted using non-linear regression. Only the Henry, Langmuir, Freundlich, BET and Toth models can fit the data (**Figs. 1-9**) The Sips model performed best in statistical tests including root-mean-square error (RMSE), adjusted coefficient of determination (adjR^2), bias factor (BF), accuracy factor (AF), and corrected Akaike Information Criterion (AICc) (**Table 2**). This is not the same to the published work [5] using a linearized form where the Langmuir and Freundlich models best represent the biosorption and the maximum biosorption capacity for the Langmuir model Qm is 191.90 mg/g. The calculated Sips parameters k_S (l/g) value of 0.10 (95% confidence interval from 0.08 to 0.13), a maximum monolayer adsorption capacity q_{mS} (mg/g) value of 252.88 (95% C.I. from 222.13 to 283.64) and n_S (Sips model exponent) value of 1.16 (95% C.I. from 1.34 to 1.98).

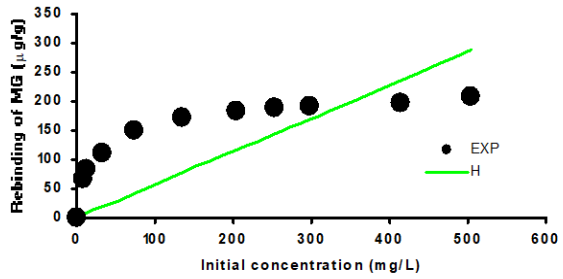

Fig. 1. Isotherm of biosorption of lead(II) onto an Antarctic sea-ice bacterial exopolysaccharide as modelled using the Henry model.

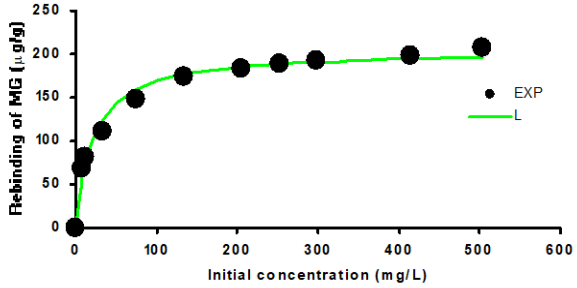

Fig. 2. Isotherm of biosorption of lead(II) onto an Antarctic sea-ice bacterial exopolysaccharide as modelled using the Langmuir model.

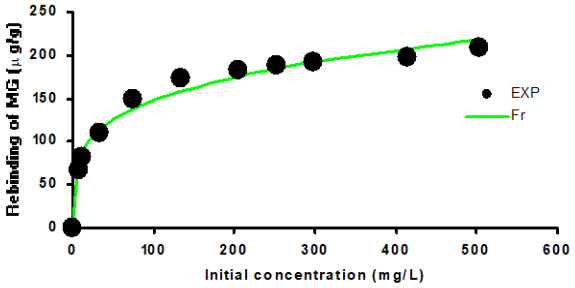

Fig. 3. Isotherm of biosorption of lead(II) onto an Antarctic sea-ice bacterial exopolysaccharide as modelled using the Freundlich model.

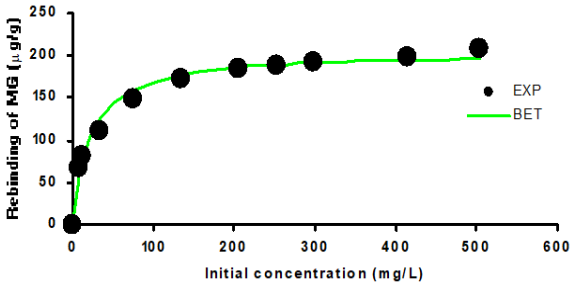

Fig. 4. Isotherm of biosorption of lead(II) onto an Antarctic sea-ice bacterial exopolysaccharide as modelled using the BET model.

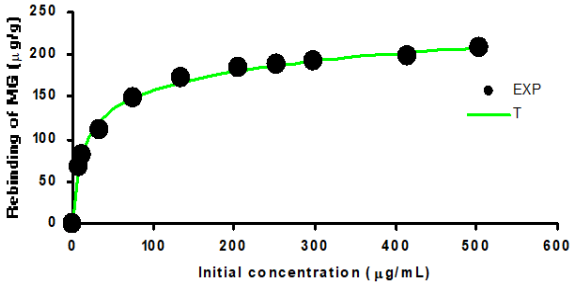

Fig. 5. Isotherm of biosorption of lead(II) onto an Antarctic sea-ice bacterial exopolysaccharide as modelled using the Toth model.

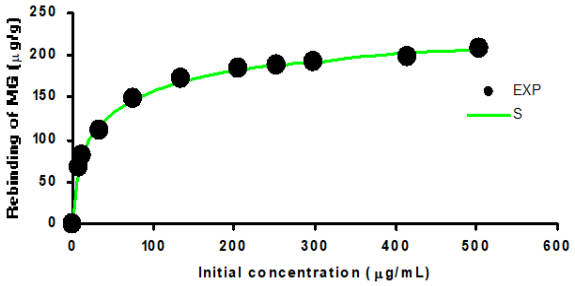

Fig. 6. Isotherm of biosorption of lead(II) onto an Antarctic sea-ice bacterial exopolysaccharide as modelled using the Sips model.

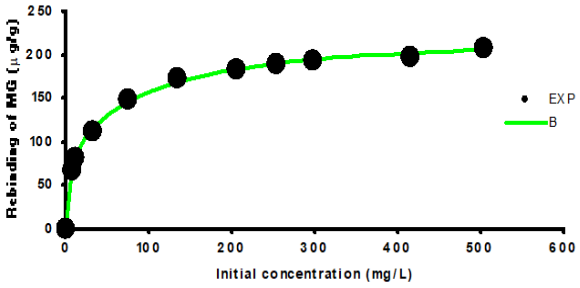

Fig. 7. Isotherm of biosorption of lead(II) onto an Antarctic sea-ice bacterial exopolysaccharide as modelled using the Baudu model.

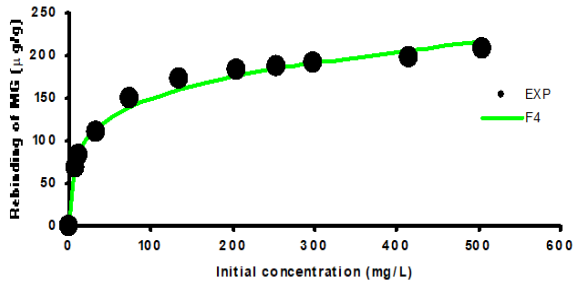

Fig. 8. Isotherm of biosorption of lead(II) onto an Antarctic sea-ice bacterial exopolysaccharide as modelled using the Fritz-Schlunder-IV model.

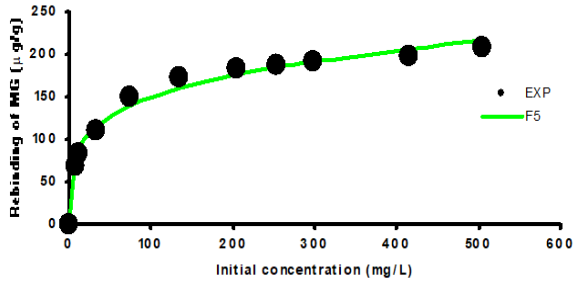

Fig. 9. Isotherm of biosorption of lead(II) onto an Antarctic sea-ice bacterial exopolysaccharide as modelled using the Fritz-Schlunder-V model.

Table 2. Error function analysis for the fitting of the isotherms of lead(II) onto an Antarctic sea-ice bacterial exopolysaccharide.

Model	*p*	RMSE	adR2	AICc	BIC	HQC	BF	AF
Henry	1	73.21	0.40	100.91	95.80	95.15	0.43	2.57
Langmuir	2	9.07	0.98	59.74	51.10	49.81	0.98	1.06
Freundlich	2	9.45	0.98	60.63	52.00	50.70	1.01	1.06
BET	3	9.62	0.98	66.97	53.50	51.56	0.98	1.06
Toth	3	4.71	0.99	51.25	37.77	35.83	1.00	1.02
Sips	**3**	**3.40**	**1.00**	**44.10**	**30.63**	**28.69**	**1.00**	**1.02**
Baudu	4	3.27	1.00	51.06	30.65	28.06	1.00	1.01
F4	4	8.94	0.98	73.23	52.82	50.23	1.01	1.05
F5	5	9.71	0.97	86.35	55.34	52.10	1.01	1.05

Note:
RMSE Root mean Square Error
p no of parameters
adR^2 Adjusted Coefficient of determination
BF Bias factor
AF Accuracy factor
AICc Adjusted Akaike Information Criterion
BIC Bayesian Information Criterion
HQC Hannan–Quinn information criterion

For the purpose of predicting heterogeneous adsorption systems, Sips [23] proposed a hybrid form of the Langmuir and Freundlich isotherms. This model gets around the issue of increasing solute concentration associated with the Freundlich isotherm. It predicts a monolayer sorption capacity typical of the Langmuir isotherm at high solute concentrations but reduces to the Freundlich isotherm at low concentrations, making it incompatible with Henry's law [24].

The Sips model was also the best model for lead(II) sorption by an iron oxide/hydroxide (α,γ-FeOOH) nanoparticles [25], by a β-cyclodextrin derivative [26] and by a modified water hyacinth (*Eichhornia crassipes*) fibers [27]. It is also the best model for fitting several heavy metals such as chromium (VI) [28], nickel (II) [29], cobalt (II) [30], arsenate [31] and many other organic compounds [32–42]

CONCLUSION

Finally, the biosorption isotherm data for lead(II) onto an Antarctic sea-ice bacterial exopolysaccharide was successfully analyzed using a variety of models with one to five parameters, including the Henry, Langmuir, Dubinin-Radushkevich, Freundlich, BET, Toth, Sips, Fritz-Schlunder IV, Baudu, and Fritz-Schlunder V models. The Sips model performed best in statistical tests including root-mean-square error (RMSE), adjusted coefficient of determination (adjR^2), bias factor (BF), accuracy factor (AF), and corrected Akaike Information Criterion (AICc) which is not the same to the originally published work using a linearized form where the Langmuir and Freundlich models best represent the biosorption and the maximum biosorption capacity. The calculated Sips parameters k_S (l/g) value of 0.10 (95% confidence interval from 0.08 to 0.13), a maximum monolayer adsorption capacity q_{mS} (mg/g) value of 252.88 (95% C.I. from 222.13 to 283.64) and n_S (Sips model exponent) value of 1.16 (95% C.I. from 1.34 to 1.98).

ACKNOWLEDGEMENT

We thank the Academy of Sciences Malaysia and Sultan Mizan Antarctic Research Foundation for funding the research under the YPASM Smart Partnership Initiative 2020.

REFERENCES

1. Raviraja A, Vishal Babu GN, Sehgal A, Saper RB, Jayawardene I, Amarasiriwardena CJ, et al. Three cases of lead toxicity associated with consumption of ayurvedic medicines. Indian J Clin Biochem. 2010;25(3):326–9.
2. Alissa EM, Ferns GA. Heavy metal poisoning and cardiovascular disease. J Toxicol. 2011;2011:870125.
3. Nepalia A, Singh A, Mathur N, Pareek S. Toxicity assessment of popular baby skin care products from Indian market using microbial bioassays and chemical methods. Int J Environ Sci Technol. 2018 Nov 1;15(11):2317–24.
4. Zhang Z, Cai R, Zhang W, Fu Y, Jiao N. A novel exopolysaccharide with metal adsorption capacity produced by a marine bacterium Alteromonas sp. JL2810. Mar Drugs [Internet]. 2017;15(6). Available from: https://www.scopus.com/inward/record.uri?eid=2-s2.0-85020838645&doi=10.3390%2fmd15060175&partnerID=40&md5=69ae60a80ebcf8c4124e47071e75c699
5. Ma Y, Shen B, Sun R, Zhou W, Zhang Y. Lead(II) biosorption of an Antarctic sea-ice bacterial exopolysaccharide. Desalination Water Treat. 2012 Apr 1;42(1–3):202–9.
6. Motulsky HJ, Ransnas LA. Fitting curves to data using nonlinear regression: a practical and nonmathematical review. FASEB J Off Publ Fed Am Soc Exp Biol. 1987;1(5):365–74.
7. Tran HN, You SJ, Hosseini-Bandegharaei A, Chao HP. Mistakes and inconsistencies regarding adsorption of contaminants from

aqueous solutions: A critical review. Water Res. 2017 Sep 1;120:88–116.
8. Ridha FN, Webley PA. Anomalous Henry's law behavior of nitrogen and carbon dioxide adsorption on alkali-exchanged chabazite zeolites. Sep Purif Technol. 2009;67(3):336–43.
9. Langmuir I. The adsorption of gases on plane surfaces of glass, mica and platinum. J Am Chem Soc. 1918;40(9):1361–403.
10. Adamson AW. Physical chemistry of surfaces. New York: UMI; 1993. 664 p.
11. Sips R. On the structure of a catalyst surface. J Chem Phys. 1948;16(5):490–5.
12. Toth J. State equations of the solid-gas interface layers. Acta Chim Acad Sci Hung. 1971;69(3):311–28.
13. Brunauer S, Emmett PH, Teller E. Adsorption of gases in multimolecular layers. J Am Chem Soc. 1938;60(2):309–19.
14. Baudu M. Etude des interactions solute–fibres de charbon actif. Application et regeneration. Universite de Rennes I; 1990.
15. Fritz W, Schluender EU. Simultaneous adsorption equilibria of organic solutes in dilute aqueous solutions on activated carbon. Chem Eng Sci. 1974;29(5):1279–82.
16. Rohatgi A. WebPlotDigitizer. http://arohatgi.info/WebPlotDigitizer/app/ Accessed June 2 2014.; 2015.
17. Halmi MIE, Shukor MS, Johari WLW, Shukor MY. Mathematical modelling of the degradation kinetics of *Bacillus cereus* grown on phenol. J Environ Bioremediation Toxicol. 2014;2(1):1–5.
18. Khare KS, Phelan Jr FR. Quantitative comparison of atomistic simulations with experiment for a cross-linked epoxy: A specific volume–cooling rate analysis. Macromolecules. 2018;51(2):564–75.
19. Akaike H. New look at the statistical model identification. IEEE Trans Autom Control. 1974;AC-19(6):716–23.
20. Burnham KP, Anderson DR. Model Selection and Multimodel Inference: A Practical Information-Theoretic Approach. Springer Science & Business Media; 2002. 528 p.
21. Kass RE, Raftery AE. Bayes Factors. J Am Stat Assoc. 1995 Jun 1;90(430):773–95.
22. Ross T, McMeekin TA. Predictive microbiology. Int J Food Microbiol. 1994;23(3–4):241–64.
23. Sips R. Combined form of Langmuir and Freundlich equations. J Chem Phys. 1948;16(429):490–5.
24. Sivarajasekar N, Baskar R. Adsorption of basic red 9 onto activated carbon derived from immature cotton seeds: isotherm studies and error analysis. Desalination Water Treat. 2014 Dec 6;52(40–42):7743–65.
25. Rahimi S, Moattari RM, Rajabi L, Derakhshan AA, Keyhani M. Iron oxide/hydroxide (α,γ-FeOOH) nanoparticles as high potential adsorbents for lead removal from polluted aquatic media. J Ind Eng Chem. 2015 Mar 25;23:33–43.
26. Zhang M, Zhu L, He C, Xu X, Duan Z, Liu S, et al. Adsorption performance and mechanisms of Pb(II), Cd(II), and Mn(II) removal by a β-cyclodextrin derivative. Environ Sci Pollut Res. 2019 Feb 1;26(5):5094–110.
27. Neris JB, Luzardo FHM, Santos PF, de Almeida ON, Velasco FG. Evaluation of single and tri-element adsorption of Pb2+, Ni2+ and Zn2+ ions in aqueous solution on modified water hyacinth (Eichhornia crassipes) fibers. J Environ Chem Eng. 2019 Feb 1;7(1):102885.
28. Divband Hafshejani L, Mortazavi P, Sabz ALiPour S, Brooman Nasab S. Isotherm and Kinetics Study of The Adsorption of Chromium (VI) From Aqueous Solution by Zizyphus Spina-christi Leaves Ash Nanoparticles. Irrig Sci Eng. 2016 Dec 21;39(4):97–110.
29. Bellaloui M, Metouchi A, Foukrache A, Larabi S, Semaoune F. Retention of a heavy metal by marl collected from aquifer substratum. Arab J Geosci. 2017 Oct 2;10(19):425.
30. Anirudhan TS, Deepa JR, Christa J. Nanocellulose/nanobentonite composite anchored with multi-carboxyl functional groups as an adsorbent for the effective removal of Cobalt(II) from nuclear industry wastewater samples. J Colloid Interface Sci. 2016 Apr 1;467:307–20.
31. Veličković ZS, Marinković AD, Bajić ZJ, Marković JM, Perić-Grujić AA, Uskokovic PS, et al. Oxidized and Ethylenediamine-Functionalized Multi-Walled Carbon Nanotubes for the Separation of Low Concentration Arsenate from Water. Sep Sci Technol. 2013 Sep 2;48(13):2047–58.
32. Mondal S, Sinha K, Aikat K, Halder G. Adsorption thermodynamics and kinetics of ranitidine hydrochloride onto superheated steam activated carbon derived from mung bean husk. J Environ Chem Eng. 2015 Mar 1;3(1):187–95.
33. Pasalari H, Ghaffari H, Mahvi A, Pourshabanian M, Azari A. Activated carbon derived from date stone as natural adsorbent for phenol removal from aqueous solution. DESALINATION WATER Treat. 2017 Jan 1;72:406–17.
34. Awadallah-F A. Adsorptive Removal of Malachite Green Chloride and Reactive Red-198 from Aqueous Solutions by Using Multiwall Carbon Nanotubes-Graft-Poly (2-acrylamido-2-methyl-1-propanesulfonic acid). J Polym Environ. 2017 Jun 1;25(2):258–76.
35. da Rosa ALD, Carissimi E, Dotto GL, Sander H, Feris LA. Biosorption of rhodamine B dye from dyeing stones effluents using the green microalgae Chlorella pyrenoidosa. J Clean Prod. 2018 Oct 10;198:1302–10.
36. Lu Y, Lim L, Priyantha N. Chemical modification of pomelo leaves as a simple and effective way to enhance adsorption toward methyl violet dye. Desalination Water Treat. 2020 Jan 1;197:379–91.
37. Saadi Z, Fazaeli R, Vafajoo L, Naser I. Adsorptive removal of apramycin antibiotic from aqueous solutions using Tween 80-and Triton X-100 modified clinoptilolite: experimental and fixed-bed modeling investigations. Int J Environ Health Res. 2020 Sep 2;30(5):558–83.
38. Khadir A, Motamedi M, Negarestani M, Sillanpää M, Sasani M. Preparation of a nano bio-composite based on cellulosic biomass and conducting polymeric nanoparticles for ibuprofen removal: Kinetics, isotherms, and energy site distribution. Int J Biol Macromol. 2020 Nov 1;162:663–77.
39. Rahdar S, Rahdar A, Ahmadi S, Zafar MN, Mohamadi L, Labuto G, et al. Removal of sulfonated azo reactive red 198 from water by CeO2 nanoparticles. Environ Nanotechnol Monit Manag. 2020 Dec 1;14:100384.
40. Wernke G, Fernandes Silva M, Silva EA da, Fagundes-Klen MR, Suzaki PYR, Triques CC, et al. Ag and CuO nanoparticles decorated on graphene oxide/activated carbon as a novel adsorbent for the removal of cephalexin from water. Colloids Surf Physicochem Eng Asp. 2021 Oct 20;627:127203.
41. Tangarfa M, Hassani NSA. Experimental stuy of tannic acid adsorption on fluorite surface: particle size effect and isotherm modelling. In: 2022 2nd International Conference on Innovative Research in Applied Science, Engineering and Technology (IRASET). 2022. p. 1–4.
42. de Morais Pinos JY, de Melo LB, de Souza SD, Marçal L, de Faria EH. Bentonite functionalized with amine groups by the sol-gel route as efficient adsorbent of rhodamine-B and nickel (II). Appl Clay Sci. 2022 Jun 15;223:106494.